Molecular Dynamics Simulations of Poly(ethylene oxide)/LiI Melts. 1. Structural and Conformational Properties

Oleg Borodin and Grant D. Smith*

Department of Chemical and Fuels Engineering and Department of Materials Science and Engineering, University of Utah, Salt Lake City, Utah 84112

Received May 27, 1998; Revised Manuscript Received August 21, 1998

ABSTRACT: Molecular dynamics (MD) simulations of PEO/LiI melts at 363 and 450 K for the ether oxygen (EO)/LiI compositions 48:1, 15:1, and 5:1 have been performed. An explicit atom quantum-chemistry-based force field developed in our previous work was used. The Li^+ cation environment from our MD simulations was found to be in good agreement with neutron diffraction isotopic substitution (NDIS) experiments performed on the EO/Li = 5:1 system. Cation complexation was found to be strongly temperature dependent. The Li^+ cations have a tendency to be coordinated by six or more contiguous EO from a single chain at the lower temperature (363 K), but as temperature increases, coordination by shorter contiguous ether oxygen atom sequences becomes increasingly probable. The number of "free" ions was found to decrease with increasing temperature, consistent with results from Raman spectroscopy experiments on similar polymer electrolyte systems. The strong temperature dependence of the cation environment indicates the importance of entropic factors in cation complexation. In contrast to the strong temperature dependence, simulations revealed the local Li^+ environment at 450 K to be nearly independent of salt concentration for systems more dilute than 15:1. In this dilute regime, the system forms salt-rich and pure PEO-like domains of size comparable to that of half of the simulation box. The Li^+ cations strongly perturb the conformations of PEO compared to those of the pure melt but only locally. It was found that addition of salt leads to a decrease of the radius of gyration of PEO chains. This effect is more pronounced at lower temperature. At higher salt concentration, the Li^+ cation environment becomes composition dependent, and the local heterogeneities begin to disappear.

Introduction

Solid polymer electrolytes are ionically conducting, solvent-free materials usually composed of alkali salts dissolved in a polymer matrix. These systems can combine the desirable mechanical properties of polymers (e.g., ease of fabrication, low density, flexibility, etc.) with good conductivity at elevated temperatures. The idea to employ polymer electrolytes for solid-state rechargeable batteries had excited considerable interest in these materials from both the applied and fundamental viewpoints.[1−5]

A major limitation for widespread application of solid polymer electrolytes is their low conductivity at ambient temperatures. A basic understanding of ionic transport mechanisms would greatly facilitate the development of new high-conductivity electrolytes. For a material to exhibit high ionic conductivity, it is necessary to optimize the number and nature of the charge carriers ("free" ions and clusters of ions with net charge). In order for charge carriers to exist, the cation−polymer binding energy should be comparable to the cation−anion binding energy; that is, the salt must dissolve in the polymer matrix. There are three major interrelated factors that play a paramount role in ionic charge transport: cation−anion complexation, cation−polymer host and anion−polymer host complexation, and the mobility of both the charge carriers and the polymer. The complexation characteristics of poly(ethylene oxide) (PEO)/LiI as a function of temperature and salt concentration are considered in this manuscript, while ion and polymer mobility will be dealt with in an upcoming paper.

Previous Studies

Recently, there have been a number of simulation as well as experimental studies targeted toward understanding the influence of cation and anion environments on conductivity mechanisms of alkali metal salts in PEO and the structurally similar poly(propylene oxide) (PPO). The structure of crystalline PEO/alkali salt systems, for example, PEO/$LiCF_3SO_3$,[6] PEO/NaSCN,[7] PEO/NaI,[8] and PEO/$NaClO_4$,[9] has been a subject of several crystallographic studies. An overall stoichiometry, given by the ratio of the concentration of ether oxygen atoms (EO) to Li^+ cations, of EO/Li = 6:1 has been observed for PEO/Li^+ (PEO/$LiClO_4$, PEO/$LiAsF_6$, etc.) crystalline complexes by Robitaille[10] et al. in the course of their studies of phase diagrams of PEO/alkali salt systems. For PEO/LiI, a crystalline phase with a stoichiometry of 3:1 has been observed.[11] Conformations of crystalline PEO and PEO/salt complexes have been summarized in ref 13. Because ion diffusion takes place mainly in the amorphous phase,[12] we will be concerned only with amorphous polymer/salt structure. However, it is helpful to consider the complexation of Li^+ in amorphous PEO in light of the structure of crystalline PEO/salt complexes, as demonstrated below.

PEO/MX (M = alkali cation, X = monovalent ion) crystals and melts have been the subject of several spectroscopic studies.[13−15] These studies indicate that the conformations of polymer chains change upon complexation. In one of the first Raman spectroscopy studies of doped PEO, Papke et al.[16] assigned the *tgttg′t* conformation to the EO/Na = 4.5:1 crystalline complex of PEO/NaX (X = Br, I, SCN, BF_4). A number of Raman and infrared spectroscopy studies have been conducted on amorphous PEO and PPO and their low-molecular-weight oligomers doped with various salts, including diglyme/$LiCF_3SO_3$,[15] PEO oligomers/(Li, Na, K− $LiCF_3SO_3$),[14] 1,2-dimethoxyethane (DME)/lithium salts,[17] and diglyme/$LiCF_3SO_3$[15] as well as PPO/$NaCF_3SO_3$,[18−20] PPO/$LiClO_4$,[18,21,22] 1,2-dimethoxypropane (DMP)/LiC-

10.1021/ma980838v CCC: $15.00
Published on Web 10/20/1998

lO_4,[22] PPO/$LiCF_3SO_3$,[23] and PPO/(LiSCN, NaSCN, KSCN, $LiBF_4$).[21] These studies reveal the emergence of new bands in the spectra, which increase in magnitude with increasing salt content. In PEO, this band has been attributed to the emergence of a "new conformer" and was assigned to distorted *tgt* and/or *tgg* conformers that are assumed to be less populous in the pure polymer.

Raman and IR spectroscopies are also capable of probing the complexation state of polyatomic anions. In polymer electrolyte systems, it has been observed that the number of "free" ions decreases with increasing temperature. Cations tend to form pairs and aggregates with anions at temperatures significantly above T_g or at high salt concentrations.[18,19] In Raman studies of PPO/$LiClO_4$ and PPO/$NaCF_3SO_3$,[18,24] as well as PEO/$LiCF_3SO_3$,[25−27] it was also found that the population of "free" ions and ion pairs exhibits only a very weak concentration dependence in salt-dilute systems.

Carlsson et al.[28] conducted neutron diffraction and QENS experiments on PPO/$LiClO_4$. Observed ordering in the static structure factor was attributed to increased local density induced by O−Li coordination. Dynamically, the segmental motion of polymer chains is slowed by solvated ions and had a characteristic time of 10^{-9} s. Neutron diffraction isotopic substitution (NDIS) experiments[29] have been performed on amorphous PEO/LiI at 363 K and will be discussed below.

It has been noted in many recent experimental studies that polymer electrolytes at low salt concentrations can be inhomogeneous on the microscopic scale, while remaining optically clear. For example, in DSC studies of PPO/NaI, PPO/$NaClO_4$, and PPO/LiX[30,31] (X = Br, ClO_4, CF_3SO_3) two separate glass transitions were observed for salt concentrations less than EO/Li = 10:1 for PPO/LiX, less than EO/Na = 10:1 for PPO/$NaClO_4$, and less than EO/Na = 13:1 for PPO/NaI. Only a single glass transition was observed for higher concentrations. In photon correlation studies[32,33] of poly(propylene glycol)/$NaCF_3SO_3$ and poly(propylene glycol)/$Mg(ClO_4)_2$, two structural relaxation processes clearly separated in time were observed. The slow process was attributed to segmental motion around cation transient cross-links, whereas the fast process was attributed to the motion of chain sequences away from the cross-links. Only dilute systems were considered in the photon correlation studies. These studies (DSC, light scattering and Raman spectroscopy[18]) suggest that microphase separation occurs in PPO for salt concentrations less than about one cation per 10 EO and that the composition of the salt-rich phase does not change in this concentration range.

Several molecular dynamics (MD) simulations of PEO/MX (MX = NaI, LiI, LiBr, $ZnBr_2$) melts have also been performed.[34−41] Important qualitative information regarding structure and conductivity mechanisms in PEO/MX systems has resulted from these simulations. However, we believe that because of the various approximations invoked in these simulations, simulations employing improved models and potential energy functions can provide significant new insight. For example, the authors in refs 34 and 35 had to increase the dielectric constant in their force field in order to observe dynamics on the time scale of their simulations, resulting in unrealistically high conductivity. Neyertz et al.[36] stated that calculation of conductivity is inconclusive for their short simulations, and the amount of I^- anions coordinated around a Na^+ cation was found to decrease slightly for the EO/Na = 20:1 system with increasing temperature. This result contradicts the Raman spectroscopy studies (listed above), which indicate an increase in anion−cation association with increasing temperature. Although an increase in anion−cation association with increasing temperature was obtained in MD simulations of PEO/NaI by Catlow et al.,[38] their systems were not completely equilibrated and therefore the simulation results should be treated only as qualitative. In ref 37 a system containing only one cation and no anions was used, thereby ignoring the important effects of anion−cation pairing and aggregates.

In this work, we report on results of MD simulations of PEO/LiI using a realistic atomistic quantum-chemistry-based force field without modifications intended to increase dynamics. Following thorough equilibration of our systems, we have performed trajectories of sufficient length to allow extraction of static and dynamic properties of the systems. The static properties of the system are considered here, while in a future paper we will report on dynamic properties. Where experimental data are available, we make quantitative comparisons with simulations. In other cases, we demonstrate that the results of our simulations are qualitatively consistent with those of experimental investigations of related systems. Given the quantitative and qualitative agreement between simulations and experiment, we can confidently glean important information regarding the mechanisms of lithium salt complexation and conductivity in PEO from our simulations.

Force Field and Methodology

Details of the simulation methodology and the quantum-chemistry-based force field are given in refs 29, 34, and 35. MD simulations were performed on PEO/LiI melts consisting of 32 CH_3-capped PEO chains composed of 12 repeat units ($H(CH_2OCH_2)_{12}H$), at three compositions (EO/Li = 5:1, EO/Li = 15:1, and EO/Li = 48:1 (ratios are rounded), corresponding to 77, 25, and 8 LiI molecules per simulation box) and at two temperatures (363 and 450 K). The constant-temperature method of Nose[36] and the Shake algorithm[37] for bond constraints were implemented, while valence angle bends and torsions remained flexible. A time step of 1 fs was used.

The systems were prepared in the following way: (i) The equilibrated pure PEO system at 450 K was taken after the final run from our previous PEO melt simulations.[42] (ii) Seventy-seven Li^+ and I^- ions with van der Waals radii equal to zero were placed at random positions in the system, and the ions were allowed to grow to their actual van der Waals radii during 100 ps at constant pressure. (iii) This system (EO/Li = 5:1) was equilibrated for 2 ns at 450 K. (iv) The low-salt-concentration systems (EO/Li = 15:1 and EO/Li = 48:1) were created from the high-salt-concentration system (EO/Li = 5:1) by randomly removing 50 and 69 Li^+ cations and I^- anions, respectively. (v) Subsequently, all three systems were equilibrated for about 3 ns. (vi) After equilibration at 450 K, the temperature of two systems (EO/Li = 5:1 and EO/Li = 15:1) was reduced to 363 K, followed by 3 ns of additional equilibration.

The simulations were performed at a constant volume chosen so as to maintain average pressures of 1 atm. Production runs were about 3 ns (4 ns for the EO/Li = 48:1 system at 450 K). A system was considered to be

in equilibrium when the rate of ion dissociation events was equal to the rate of ion association, and average conformational populations of PEO chain sequences and the average radius of gyration of PEO chains were constant with time.

A quantum-chemistry-based force field, used in previous simulations of pure PEO melt,[45] was employed to describe the polymer/polymer interaction. The densities of the PEO melt system, characteristic ratios of PEO chains, and ^{13}C NMR spin lattice relaxation times were reported in the previous work[38,42] and were in good agreement with experimental values. The ion/ion and ion/polymer force fields were obtained from ab initio quantum chemistry studies of complexes of methane and model ethers with Li^+ and I^- ions.[46] Ion/ion and ion/polymer polarization effects were described using a two-body polarization model.[46] The effective ion and atomic polarizabilities were determined by fitting to the quantum chemistry ion/ion and ion/ether complex energies. The influence of effective ion and atomic polarizabilities on the local cation environment was investigated in our previous work.[29] An accurate description of the effective polarizabilities was found to be essential for the correct representation of the local cation environment.

Local Cation Environment

Pair Correlations. It is generally accepted that the mechanism of ionic transport in polymer electrolytes depends strongly upon the cation environment. Therefore, an accurate reproduction of structural properties is mandatory for a quantitative description of conduction. Quantitative information about the Li^+ environment can be obtained from neutron diffraction experiments on two polymer electrolyte systems that differ only in the isotope of the cation. The difference between the structure factors for these systems is a function of cation−anion, cation−cation, and cation−polymer atoms spatial correlations only. Results of such a neutron diffraction isotopic substitution (NDIS) experiment on a PEO/LiI system at 363 K and EO/Li = 5:1 have been reported.[29] The partial radial distribution function $\Delta g(r)$ obtained from NDIS is given by

$$\Delta g(r) = 0.124 g_{Li-O}(r) + 0.284 g_{Li-C}(r) + 0.572 g_{Li-H}(r) + 0.023 g_{Li-I}(r) + 0.001 g_{Li-Li}(r) \quad (1)$$

for a EO/Li = 5:1 composition. The coefficients for the various pair distribution functions are determined by the neutron-scattering length and the number density of the species. Note that contributions from Li−Li and Li−I correlations are negligibly small and that, therefore, $\Delta g(r)$ mainly reflects the spatial correlation resulting from Li^+ complexation by PEO.

$\Delta g(r)$ values from NDIS measurements with MIN errors and from MD simulations are compared in Figure 1. (MIN is the minimum noise technique used to Fourier transform the experimental q-space function.[29]) The cation environment obtained from our simulations is in excellent agreement with the NDIS experiments. The first peak in $\Delta g(r)$ from our MD simulations and from the NDIS experiments occurs at 2.07 Å and, according to our simulation pair distribution functions, is due to Li−O correlations. This close approach of Li^+ cation and oxygen is the result of strong electrostatic and polarization interactions, and an accurate representation of these interactions is required in order to reproduce experiment. For example, previous simulations[34,35] where the electrostatic interactions were reduced by a factor of 3 yield a Li−O peak at about 2.35 Å, much greater than is seen experimentally. Our simulations indicate that the position of the first Li−O peak is nearly independent of temperature and composition. Therefore, it is interesting to compare the position of the first Li−O peak from our simulations with the average Li−O distance in crystalline complexes. In PEO/$LiCF_3SO_3$ with EO/Li = 3:1[9] the average (nearest neighbor) Li−O distance was 2.04 Å.

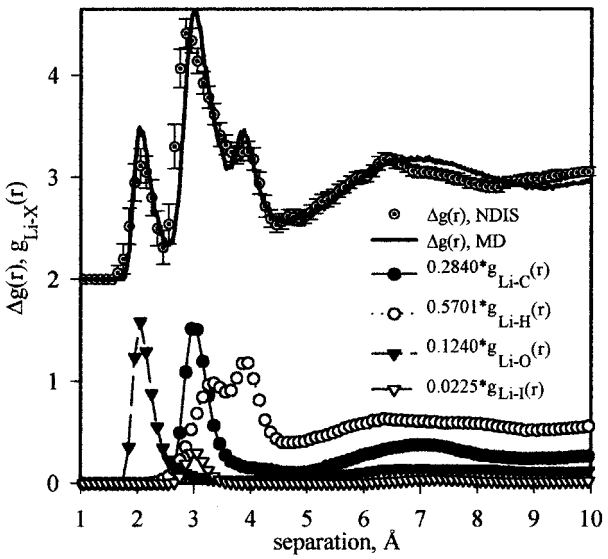

Figure 1. $\Delta g(r)$ for the EO/Li = 5:1 PEO/LiI system at 363 K from MD simulations and NDIS experiments with MIN error bars, offset by 2.0. The most important (weighted) pair distribution functions $g_{Li-X}(r)$ contributing to $\Delta g(r)$ obtained from the MD simulations are also shown.

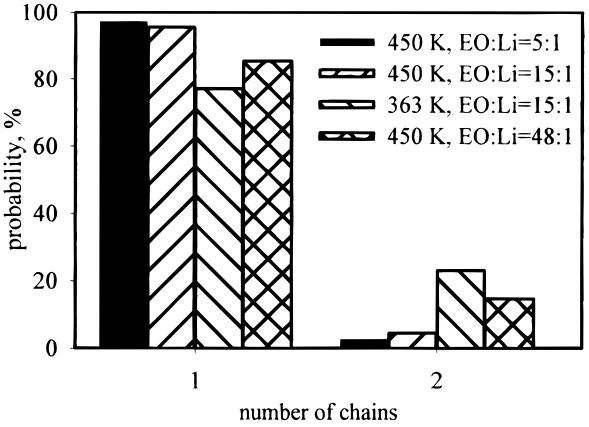

Figure 2. Probability of a Li^+ cation being complexed by one or two PEO chains.

Li^+/PEO Complexation. It has been suggested in the literature that effective transient cross-linking of PEO chains is formed by means of coordination of a Li^+ cation by more than one chain. Although such transient cross-linking events were seen in our simulations, they are rare at 450 K. The probability of finding a Li^+ cation complexed by one or two different chains is shown in Figure 2 for 450 K. The overwhelming majority of Li^+ cations are complexed by oxygen atoms from a single chain. The probability of a Li^+ cation being complexed by more than one chain increases with decreasing temperature. It is interesting that from consideration of the temperature dependence of the Brillouin fre-

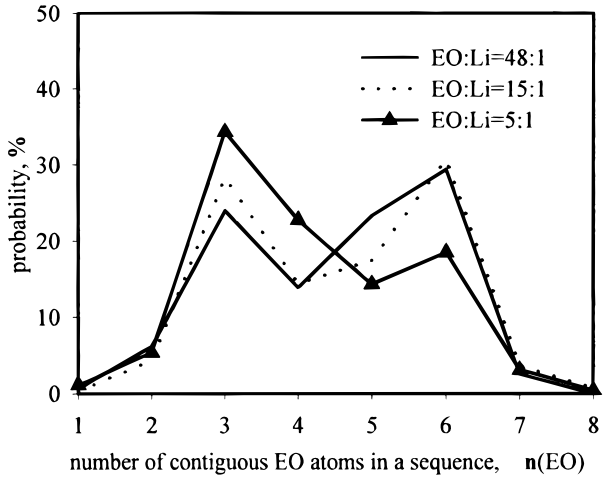

Figure 3. Composition dependence of the probability of an ether oxygen atom participating in a sequence of *n* contiguous ether oxygen atoms coordinating a Li^+ cation at 450 K.

quency shift for CH_3-capped low-molecular-weight PEO/$LiCF_3SO_3$ systems Torell et al.[53] have suggested that the number of transient cross-linking centers increases with decreasing temperature.

The question of how many ether oxygen atoms participate in complexation of a Li^+ cation was partially answered in our previous work.[29] NDIS measurements as well as our MD simulations yield an average of 3.5 ether oxygen atoms within 3.0 Å of each Li^+ for (PEO)/LiI with EO/Li = 5:1 at 363 K. A more detailed examination of our simulation results reveals a wide distribution of complexation environments, with a significant probability of finding anywhere from 2 to 7 ether oxygen atoms in the first coordination shell of a Li^+ cation, with 3 and 6 EO being the most probable. The probability of an ether oxygen participating in a sequence of *n*(EO) within the 4.0 Å complexation shell of a Li^+ cation is shown in Figure 3**.** Note that the composition dependence becomes significant only for compositions greater than 1 Li^+ cation per 15 ether oxygen atoms. The temperature dependence of the complexation environment will be considered below.

Influence of Li^+ Cations on PEO Conformations

It has been observed in numerous Raman and infrared spectroscopy measurements that MX salts significantly influence conformations of polyethers (see Introduction). Although interpretations of the spectra suggest that the populations of *tgt* and *tgg* conformational triads (−C−O−C−C−O−C− dihedral sequences) increase with increasing salt concentration, absolute conformer populations cannot be deduced from such experiments. To compare simulation predictions with experiments and to understand more quantitatively the influence of Li^+ cations on polymer conformations, we have calculated the populations of the most populous conformational triads as a function of salt concentration (Figure 4). Only the populations of the *tgt* and *tgg* conformers increase with increasing salt content, while all other important melt conformers (*ttt, ttg, tgg′*) decrease in population. As we noted in previous work,[46] Li^+ cations can favorably interact with both ether oxygen atoms in *tgt* and *tgg* triad conformations, while, in the other important melt conformations, Li^+ can bind strongly to only one of the ether oxygen atoms in the triad, resulting in lower complex energies.

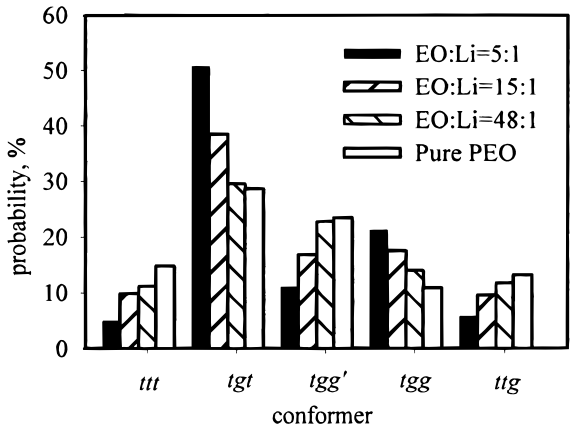

Figure 4. Composition dependence of the populations of the most important conformational triads at 450 K. The populations of the conformational triads in the pure PEO melt at 450 K are also shown.

Figure 4 illustrates that as the concentration of salt increases, the populations, and hence the relative free energies, of the conformers change due to interactions of the polymer with the Li^+ cations. We are particularly interested in the relative strength of the interactions of the various conformers with Li^+ cations, which is quantified by the change in the relative free energies of the conformational triads upon complexation. We begin by examining only those triads that are directly involved in Li^+ cation complexation. For this purpose, a "triad" was considered to be complexed if at least one of its ether oxygen atoms had at least one Li^+ cation within 4.0 Å. The free energies of the complexed conformational triads at 450 K relative to the complexed *ttt* triad can be determined using the relationship

$$\Delta A_i = -RT \ln\left(\frac{g_{ttt}p_i}{g_i p_{ttt}}\right) \qquad (2)$$

where $i = \{tgt, ttg, ttt, tgg', \text{and } tgg \text{ conformers}\}$, g_i is the degeneracy of the conformer (e.g., $g_{ttt} = 1$, $g_{tgt} = 2$), p_i is the population of conformer *i among complexed triads*, *T* is the temperature, and *R* is the universal gas constant. If we subtract from ΔA_i the quantity ΔA_i^{melt}, the relative free energy of the conformers in the pure melt (determined from eq 2 using the pure melt populations), we obtain $\Delta A_i^{\text{complex}}$. This latter quantity, shown in Figure 5 as a function of the system composition, is the relative change in conformational free energy upon complexation per complexed triad. A negative change in the conformational free energy $\Delta A_i^{\text{complex}}$ indicates stabilization of a conformer upon salt complexation relative to the *ttt* conformer. The two conformers (*tgt, tgg*) that allow a Li^+ cation to be strongly complexed by both EO have the highest stabilization energy (about 2.0 kcal/mol). The other two important melt conformers (*ttg, tgg′*) were stabilized relative to *ttt* by only 0.5 kcal/mol. Note that the *ttt* conformer is the only important conformer with no permanent dipole moment and has the weakest interaction with Li^+ cations.

The stabilization energies $\Delta A_i^{\text{complex}}$ of the conformational triads exhibit only very weak composition dependence. The populations of the uncomplexed, or free, conformational triads are also independent of composition and are the same as their populations in the pure melt (not shown). This means that the influence of Li^+ cation on PEO conformations is very local and therefore

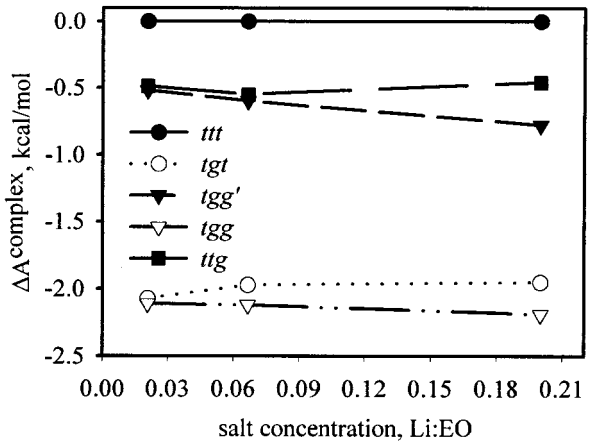

Figure 5. Stabilization energies for the most important conformational triads upon salt complexation at 450 K.

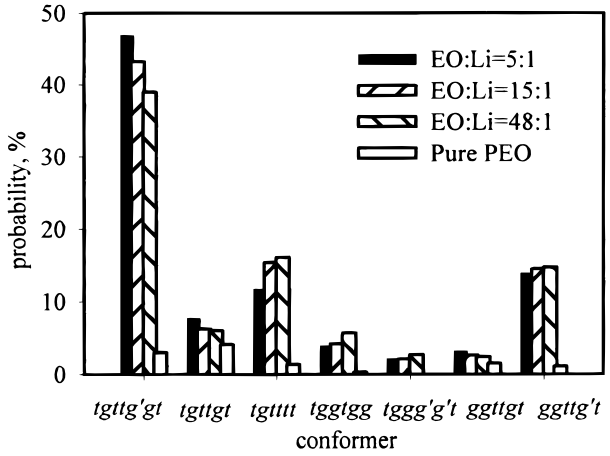

Figure 6. Composition dependence of the populations of the most important complexed conformational sextets at 450 K. The populations of the conformational sextets in the pure PEO melt at 450 K are also shown.

that the total conformational populations can be represented as a weighted sum of populations of complexed and free conformers.

Conformational Sextets. It was shown in Figure 3 that Li^+ cations are only occasionally complexed by just two consecutive EO, corresponding to a conformational triad. One of the most probable scenarios of Li^+ cation complexation at 450 K involves sequences of three EO, corresponding to a sequence of six dihedrals −C−O−C−C−O−C−C−O−C− (a conformational sextet). The most probable configurations of a complexed sextet are shown in Figure 6 at 450 K**.** Populations of the conformational sextets in the pure PEO melt were also calculated and are shown in Figure 6. The most probable sequence for the complexed sextet is *tgttg′t*. It is of interest to note that the same torsional angle sequence was determined by Parpke et al.[16] to be the most populated conformer from their Raman and infrared studies of $(PEO)_{4.5}NaX$ crystalline complexes, where (X = Br, I, SCN, BF_4).

Note that two of the important melt conformations, *ggttgt* and *tgttgt*, have unfavorable interactions with Li^+ cations relative to those of the other important melt conformations. The latter conformer corresponds to the conformation of the pure polymer in the crystalline state. The relatively unfavorable interaction of these conformers with Li^+ cations is due to the fact that these conformers must undergo significant distortions of their

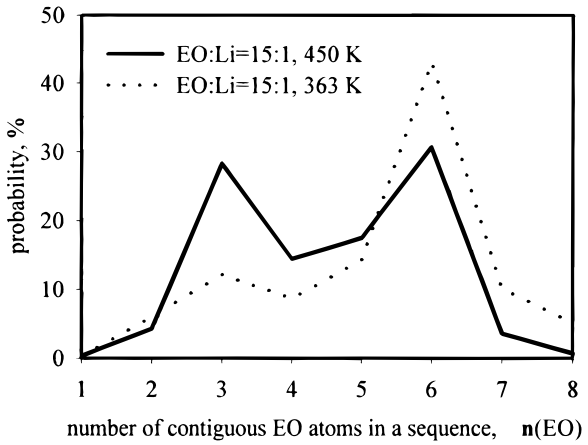

Figure 7. Temperature dependence of the probability of an ether oxygen atom to participating in a sequence of *n* contiguous ether oxygen atoms coordinating a Li^+ cation for EO/Li = 15:1.

torsional angles in order to maximize favorable EO−Li^+ interactions. In their optimized complexed configuration, the central O−C and C−O torsions for these conformers were about 164°, corresponding to nearly 20° distortion from a true trans conformation. Unlike these conformers, the $\phi_1$gttg′ϕ_6 conformers do not have to undergo major conformational distortions in order to adopt a favorable binding geometry with Li^+ cations. It is therefore clear that optimization of O−Li^+ interactions is critical in determining chain conformations in PEO/Li salt systems, both amorphous and crystalline.

The relative free energies of complexation $\Delta A_i^{complex}$ can be determined for the conformational sextets analogously to the analysis for conformational triads (eq 2). As the *tgttgt* conformers have nearly the same populations in the pure melt as in the PEO/LiI solutions, we determined free energies of complexation relative to this conformation. The *ggttgt* conformations are not stabilized relative to the *tgttgt* conformer, while the *tgttg′t*, *tggtgt*, *tggtgg*, and *ggttg′t* conformers are all stabilized by about 2 kcal/mol relative to the *tgttgt* conformer upon complexation with Li^+ cations. Although the *tggg′g′t* conformers have the highest stabilization energy (3.0 kcal/mol), their population after complexation is still relatively low (about 5%) because of inherently high conformational energy.

Influence of Temperature on Conformations of PEO/Li^+ Complexes

Up to this point, we have been concerned with changes in PEO conformations and the Li^+ cation environment with increasing salt content. Here we consider the influence of temperature on the Li^+ cation environment. One of the prominent changes with temperature occurs in the distribution of contiguous ether oxygen atom sequences in the Li^+ cation coordination shell. The probability of finding an ether oxygen in a sequence of *n* contiguous EO around a Li^+ cation is shown in Figure 7 at 363 and 450 K for EO/Li = 15:1 (the composition dependence at 450 K is shown in Figure 3). To understand the driving force for these changes we have calculated the free energies for *n* contiguous EO relative to, $n = 3$, which are given in Table 1. In Figure 7, the probability of $n = 3$ decreases and the probabilities for each $n \geq 5$ increase with decreasing temperature. Table 1 shows that the relative free energies of five and six contiguous ether oxygen

Table 1. Complexing EO Sequence Probabilities and Relative Free Energies for EO/Li = 15:1 as a Function of Temperature

	T = 363 K		T = 450 K	
no. of contiguous EO	probability	ΔA,[a] kcal/mol	probability	ΔA,[a] kcal/mol
1	0.013	1.947	0.014	2.986
2	0.138	0.221	0.087	1.318
3	0.187	0.000	0.381	0.000
4	0.100	0.450	0.146	0.860
5	0.132	0.251	0.147	0.851
6	0.332	−0.413	0.207	0.546
7	0.067	0.743	0.020	2.635
8	0.029	1.336	0.004	4.120

[a] Relative to the three contiguous EO sequence.

Table 2. Temperature and Concentration Dependence of the Most Important Ether Oxygen Atom Conformational Sextets

		population, %			
		363 K	450 K		
degeneracy	conformation	15:1	15:1	48:1	5:1
4	*tgt tg′t tgt tg′g′ tg′g′*	21.7	11.0	9.8	4.5
4	*tgt tg′t tgt tg′g′ tg′t*	9.6	9.0	8.8	5.7
4	*tgg tgt tg′t tgt tg′g′*	6.7	5.0	4.4	2.9
4	*tgt tg′t tgt tg′g′ ggt*	3.4	2.8	1.5	2.8

atom sequences are about 1 kcal/mol lower at the lower temperature. For longer sequences (seven and eight contiguous EO) this difference is around 2 kcal/mol or more. This strong temperature dependence indicates that there is an important entropic contribution to the stabilization of the longer sequences with decreasing temperature.

The following picture of complexation of Li^+ cations by PEO can be drawn. Enthalpic contributions, due to strong EO−Li^+ interactions, favor complexation of Li^+ cation by long sequences of EO. At the same time, only relatively few PEO conformations allow highly favorable PEO/Li^+ cation interactions for long EO sequences. As a result, there is a large unfavorable entropic ($-T\Delta S$) contribution to the free energy of PEO/Li^+ cation complexation by longer EO sequences. At lower temperatures entropic contributions are relatively less important and the chains tend to adopt their energetically preferred longer complexing sequences. At higher temperatures the entropic penalty for these long sequences increases. Hence, the populations of shorter configurations with greater conformational entropy, but with less favorable PEO/Li^+ binding energies, increase.

The importance of entropic contributions to the complexation of Li^+ cations is further demonstrated in Table 2, which gives the population of the most important conformations of complexed sequences of six EO for various compositions as a function of temperature. At 363 K, the four most populous conformer types (16 total conformers) account for 41.4% of the total population of complexed sequences at the EO/Li = 15:1 salt composition. This is out of a total of nearly 1.5E+07 possible conformations. This contribution drops to 28% at 450 K as the remainder of configurational phase space becomes more populated.

Temperature and Composition Dependence of the Local Ion Environment

Influence of Temperature and Composition on Li^+ Coordination. The increase in the PEO/Li^+ cation relative free energy of complexation for longer EO sequences with increasing temperature has a dramatic effect on the nature of the complexation of Li^+ cations. This is demonstrated in Figures 8 and 9, where the number of EO and the number of I^- anions in the first Li^+ coordination shell are shown as a function of temperature for various compositions. For dilute concentrations (EO/Li = 48:1 and EO/Li = 15:1) the number of EO involved in Li^+ cation complexation decreases with increasing temperature, while the number of I^- anions increases. It is clear that I^- anions compete with EO in Li^+ complexation at higher temperatures, where the PEO chain is "entropically" forced to adopt shorter ether oxygen atom complexing sequences. In contrast, little temperature dependence of the local Li^+ cation environment is observed for the EO/Li = 5:1 system. This is consistent with ion saturation, as discussed below.

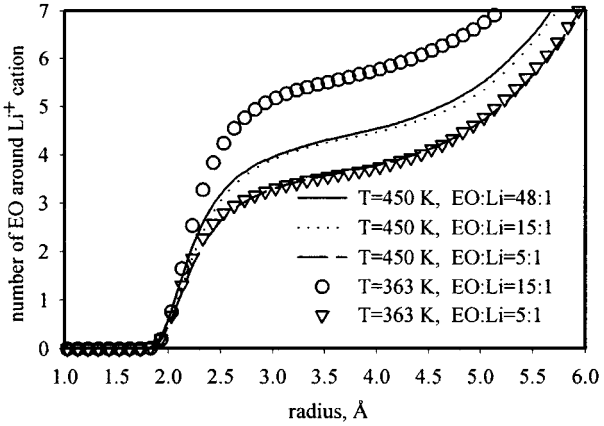

Figure 8. Composition and temperature dependence of the average number of ether oxygen atoms coordinated within the distance r of a Li^+ cation.

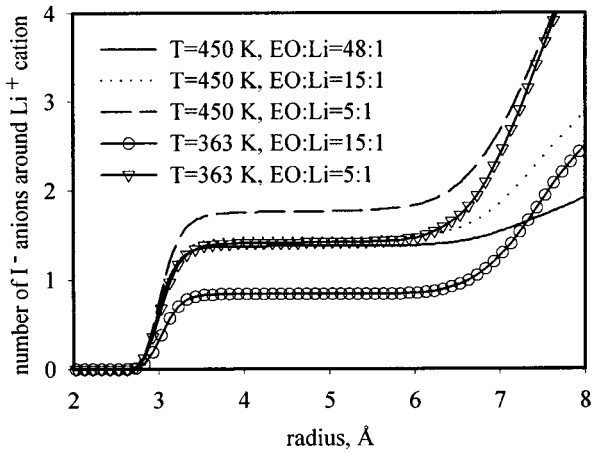

Figure 9. Composition and temperature dependence of the average number of ether iodine anions coordinated within the distance r of a Li^+ cation.

Ion−Ion Interactions. We now consider in detail the influence of temperature on cation−anion interactions, focusing on free ions, pairs, and larger aggregates. Information about "free" anions, anion−cation pairs, and aggregates can be obtained from consideration of stretching and rocking motions of polyatomic anions from Raman spectra. Triflate ($CF_3SO_3^-$) anions are one of the most suitable anions for such studies. Raman spectroscopy studies of PPO/$LiCF_3SO_3$,[18] PPO/$LiClO_4$,[18] PPO/$NaCF_3SO_3$,[18,20] and PEO/$LiCF_3SO_3$[25−27] have shown that the local ion environment, that is, relative populations of "free" ions, ion pairs, and aggregates, exhibits

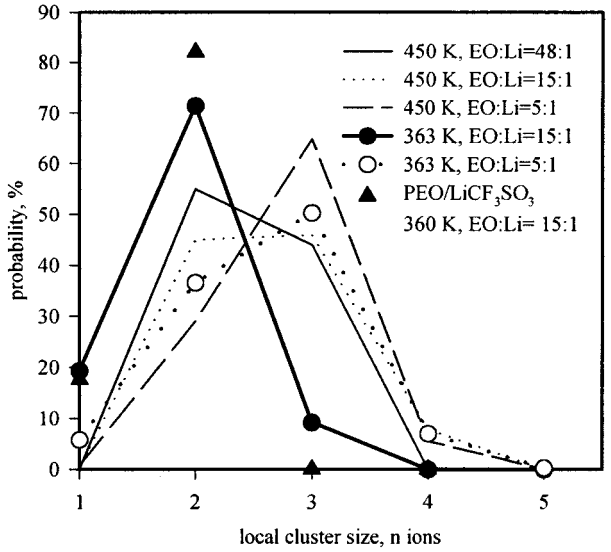

Figure 10. Temperature and composition dependence of the probability of finding $n - 1$ ions (local cluster size n) within 4.0 Å of any given ion for PEO/LiI systems. The probabilities of free ions, ion pairs and ionic aggregates for PEO/$LiCF_3SO_3$ at 360 K from Raman spectroscopy studies[26] are also shown.

only a very weak composition dependence in the composition range from EO/Li = 1000 to EO/Li = 10:1 for PPO/$LiClO_4$, from EO/Na = 1000 to EO/Na = 10:1 for PPO/$NaCF_3SO_3$, from EO/Li = 80:1 to EO/Li = 20:1 for CH_3-capped PEO(400),[25] and from EO/Li = 80:1 to EO/Li = 20:1 for 13 repeat units PEO doped with $LiCF_3SO_3$.[26] At higher salt concentrations a decrease in the fraction of "free" ions and an increase of the population of aggregates was observed. Unfortunately, such Raman spectroscopy studies are fundamentally impossible on the PEO/LiI system, but it is instructive to compare our simulation results with the above-mentioned Raman studies on similar systems, as is done below.

The probability for an ion to participate in a *local* cluster of n ions is shown in Figure 10. We considered an ion to be a member of a local cluster of size n when it has $n - 1$ other ions within 4 Å. The temperature dependence of this distribution is dramatic. For EO/Li = 15:1, we observed a substantial increase in the free ion population, while the amount of aggregates (larger than pairs) dropped below 10% upon decreasing the temperature from 450 to 363 K. For the EO/Li = 5:1 system the temperature dependence of the local ion environment is less pronounced than that for EO/Li = 15:1. Nevertheless, for EO/Li = 5:1 the number of local clusters (three) decreased while the number of free ions and ion pairs increased with a temperature decrease from 450 to 363 K. This is a direct manifestation of the earlier-mentioned increase in "free" ion population with decreasing temperature observed in many Raman and infrared studies of polymer electrolytes.[15,18,19,39] At higher temperature (450 K), we observe very few free ions. Note that phase separations ("salting out" of salts) could be thought of as a continuation of the process of increasing cation/anion pairs and aggregates with a further temperature increase. For example, precipitation of salt occurs for the PEO/NaI system (EO/Na = 16:1) at about 540 K[30] and was observed in recent MD simulations of the PEO/NaI system[40] upon an increase in temperature from 500 to 1000 K.

The composition dependence of the distribution of the local ion clusters at 450 K is also shown in Figure 10. The distributions of the local ion clusters are only slightly different for the EO/Li = 15:1 and EO/Li = 48:1 systems, while for high salt concentration (EO/Li = 5:1) a quite different distribution was obtained. We also note that at higher salt concentration, clusters of two or more ions are the most probable. These results are in accord with the above-mentioned Raman spectroscopy studies on similar systems. It is interesting to compare the local ion environment from our simulation of CH_3-capped 12 repeat unit PEO/LiI at EO/Li = 15:1 and 363 K with the local ion environment from Raman spectroscopy on the CH_3-capped 13 repeat unit PEO/$LiCF_3SO_3$ system at EO/Li = 15:1 and 360 K,[26] also shown in Figure 10.

Local Domains

The manner in which ions are distributed will have a profound effect on the mechanism of charge transport in solid polymer electrolytes. In the previous sections, we considered the local ionic environment on a length scale of 4.0 Å. Clearly the systems are heterogeneous on this scale. Particularly, the conformations of complexed PEO sequences are different from conformations of uncomplexed PEO sequences, and some ions formed ion pairs while the others participated in aggregates or exist as "free" ions. Raman spectroscopy is the most suitable technique for probing system properties on this scale, and comparison of our simulations with these experiments was considered in the previous section.

The question remains as to the existence and nature of larger-scale heterogeneities, or domains, in PEO/LiI. A domain is a region of a system having certain properties (such as atom−atom spatial correlations, conformational populations, etc.) distinct from those in another region. To obtain information about heterogeneity in the system on larger scales, experimental techniques such as differential scanning calorimetry (DSC) and photon correlation spectroscopy can be used. PPO/LiX systems, where X = Br, ClO_4, or CF_3SO_3,[30,31] have been studied by DSC. Two glass transition temperatures were observed in these experiments, while the samples remained optically clear. One process corresponded to pure PPO, while the other corresponded to the PPO/salt complex of about EO/Li = 10:1. This suggests a formation of domains at least several nanometers in size but smaller than a micron. In the same experiments a single process was observed for the PEO/NaX and PEO/LiX systems, indicating that salt-rich domains in PEO (if any) are smaller than those in PPO. The size of domains leading to two glass transitions is unclear but must be larger than a pair of salt molecules complexed by PEO because $(PEO/LiClO_4)_2$ clusters have been observed in spectroscopic studies[41] of PEO/$LiClO_4$, a system that does not exhibit two glass transitions.[30]

Evidence for domains in PEO/LiI can be seen in Figure 10 together with Figures 8 and 9 and Table 2, which indicate that the local ion environment does not change significantly with salt composition for compositions less than EO/Li = 15:1 at 450 K. Specifically, the number of iodine anions and number of EO coordinated around Li^+ cations as well as conformations of sequences of PEO chain coordinated around Li^+ cation are only slightly composition dependent. Additionally, uncomplexed PEO sequences have the same conformational populations as the pure PEO melt.[42] These data suggest the presence of salt-rich domains as well as pure PEO-like domains; that is, the system is heterogeneous on some scale.

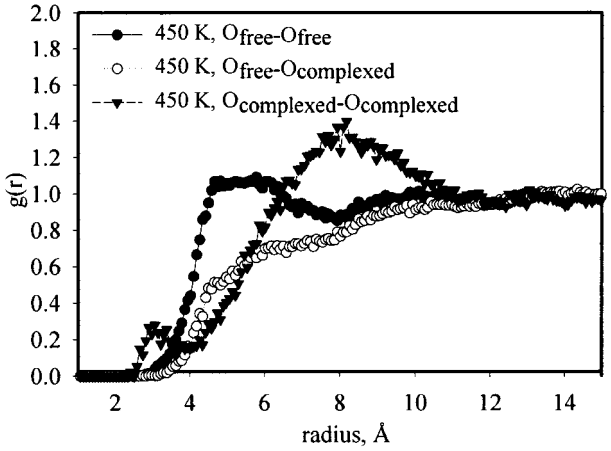

Figure 11. Intermolecular pair distribution functions for the EO/Li = 15:1 PEO/LiI system at 450 K.

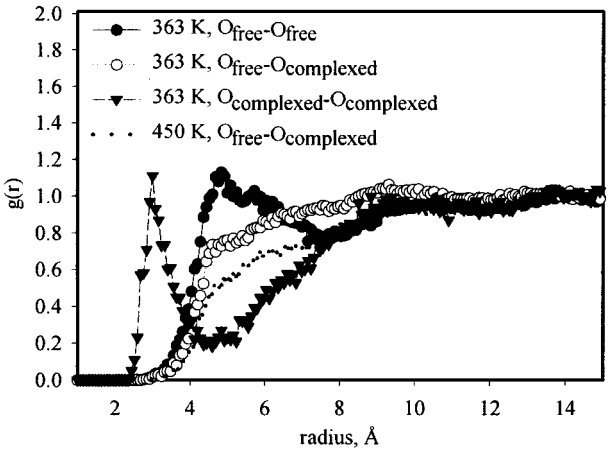

Figure 12. Intermolecular pair distribution functions for the EO/Li = 15:1 PEO/LiI system at 363 K. The $O_{free}-O_{complexed}$ intermolecular pair distribution function for EO/Li = 15:1 at 450 K is also shown.

To further address the question of local heterogeneity, we have divided all ether oxygen atoms into two categories. Ether oxygen atoms that did not lie within 4.0 Å of a Li^+ cation were labeled free ether oxygen atoms while oxygen atoms within 4.0 Å of a Li^+ cation were labeled complexed. Intermolecular pair distribution functions for $O_{free}-O_{free}$, $O_{free}-O_{complexed}$, and $O_{complexed}-O_{complexed}$ are shown in Figures 11 and 12, for EO/Li = 15:1 at 450 and 363 K, respectively. It was found that for EO/Li = 15:1 and 48:1 (not shown) the $O_{free}-O_{free}$ intermolecular pair distribution functions are essentially identical to the EO−EO intermolecular pair distribution functions from simulations of the pure PEO melt at the corresponding temperatures.[42] This is further evidence of domains in the PEO/LiI system that locally resemble pure PEO. However, this is not the case for the EO/Li = 5:1 system (not shown here), where deviations of the $O_{free}-O_{free}$ intermolecular pair distribution function from the EO−EO intermolecular pair distribution function from pure PEO melt simulations were observed.

Figures 11 and 12 reveal that the $O_{complexed}-O_{complexed}$ intermolecular pair distribution functions differ significantly from the $O_{free}-O_{free}$ intermolecular pair distribution functions. The $O_{complexed}-O_{complexed}$ intermolecular pair distribution functions at 450 K for all compositions have peaks at about 3.0 and 8.0 Å. The first peak corresponds to EO−Li^+−EO interchain transient cross-linking, and the second peak corresponds to the EO−(Li^+-I^-−Li^+)-EO type of transient cross-linking. The $O_{complexed}-O_{complexed}$ intermolecular pair distribution function changes qualitatively with a temperature drop from 450 to 363 K. Comparing Figures 11 and 12, the second peak, corresponding to the EO−(Li^+-I^-−Li^+)−EO type of transient cross-linking, disappears at the lower temperature, reflecting the very low probability of clusters of three or more ions, previously shown in Figure 10. Therefore, at 363 K, ether oxygen atoms on different chains are transiently cross-linked by means of EO−Li^+−EO.

The various O−O intermolecular pair distribution functions allow us to estimate domain size. At 450 K, Figure 11 shows that for distances greater than about 11 Å all of the O−O intermolecular pair distribution functions merge for the EO/Li = 15:1 system, indicative of random mixing on this length scale. Similar behavior is seen for the EO/Li = 48:1 system. The $O_{complexed}-O_{free}$ intermolecular pair distribution function approaches unity at this distance, indicating that identifiable domains of complexed and uncomplexed oxygen atoms do not exist on this length scale. In Figure 12 we compare the $O_{complexed}-O_{free}$ intermolecular pair distribution functions at 450 and 363 K. At the lower temperature, the function more rapidly approaches unity, indicating smaller domains. An even more rapid approach toward unity is seen for the EO/Li = 5:1 system at 450 K. For the EO/Li = 15:1 system, the smaller domains at lower temperature are due to the disappearance of ion clusters, while for the EO/Li = 5:1 system, the system is ion saturated and cannot effectively segregate into salt-rich and PEO-like domains. Taking into account the long-range nature of Coulombic forces and the relative sizes of the domains (diameter up to 22 Å at 450 K) and the simulation box (32 Å), it is possible that the domain size may increase for EO/Li compositions ≥ 15:1 if a larger simulation box were employed. We therefore estimate a lower bound for salt-rich and pure PEO-like domains of around 11 Å in radius for the lower concentrations at 450 K.

To illustrate ion clustering and domains in the system, we show representative snapshots of ion configurations for four systems in Figure 13. We have connected cations and anions when the distance between them was less than 4.0 Å. At 450 K we found many sequences of up to seven ions for EO/Li = 48:1 and EO/Li = 15:1. The ions are heterogeneously distributed, with often clearly identifiable salt-rich and pure PEO-like domains. In contrast, at 363 K only a few short ion sequences are seen, with the majority of ions existing as either ion pairs or free ions. The PEO/LiI system becomes more homogeneously mixed with a temperature drop from 450 to 363 K. The picture for EO/Li = 5:1 at 450 K is quite different. Here, a much more homogeneous "network" of often quite large ion sequences is formed.

Composition and Temperature Dependence of the PEO Radius of Gyration

As was shown above, addition of LiI has a profound effect on local PEO conformations, which should be reflected in the overall dimensions of the polymer chain, given by the radius of gyration. The temperature and composition dependence of the mean-square radius of gyration of the PEO chains is shown in Figure 14. The radius of gyration was calculated during the last 1.5 ns

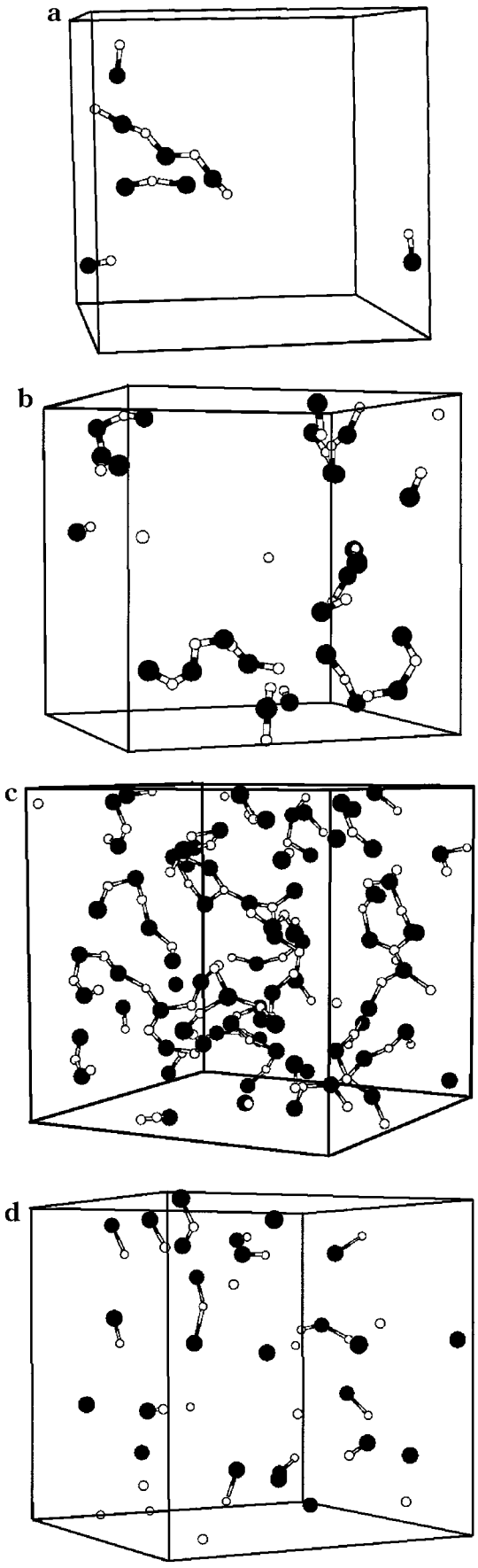

Figure 13. Instantaneous snapshots of the simulation system (only ions are shown for clarity): (a) $T = 450$ K, EO/Li = 48:1; (b) $T = 450$ K, EO/Li = 15:1; (c) $T = 450$ K, EO/Li = 5:1; (d) $T = 363$ K, EO/Li = 15:1. Ions were connected when the distance between them was less than 4.0 Å.

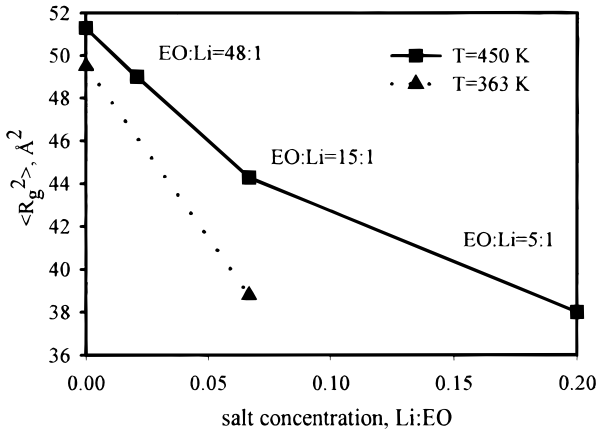

Figure 14. Temperature and composition dependence of the mean-square radius of gyration of 12-repeat-unit PEO chains.

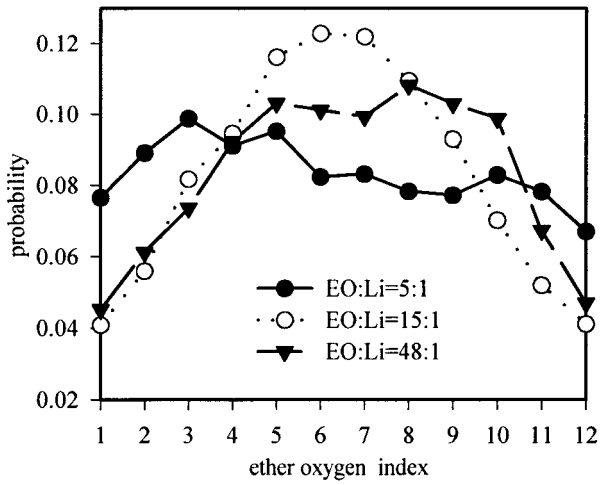

Figure 15. Composition dependence of the relative probability of an ether oxygen in a 12-repeat-unit CH_3-capped PEO chain to participate in complexation of a Li^+ cation as a function of position along the chain.

of the MD trajectories. We estimate the accuracy of our $\langle R_g^2 \rangle$ values to be ± 1 Å^2. We observe a large, nearly linear decrease in the mean-square radius of gyration with increasing salt composition for EO/Li salt concentrations $\geq$ 15:1. Note that the effect of salt on R_g is more pronounced at the lower temperature, where longer complexing EO sequences are more probable. In addition, we observe that the temperature dependence of R_g increases with increasing salt content.

Chain End Effects

We have performed our simulations using an ensemble of 12 repeat unit PEO chains; hence, chain end effects may be important in cation complexation for our systems. The relative probability of an EO to participate in Li^+ complexation is shown in Figure 15 as a function of the position of the oxygen atom along the chain. Ether oxygen atoms near the center of the PEO chain have a higher probability of participating in Li^+ complexation. As Li^+ cations tend to be complexed with three or more EO for the same chain, the EO near the center of the PEO chain can participate in more complexation events. The much weaker dependence of the probability of an EO participating in Li^+ cation complexation on the position in the chain for the EO/Li = 5:1 system is due to the fact that at this composition the majority of EO are involved in complexation and

therefore the Li^+ cation has a more limited "choice" of EO with which to complex. We can conclude that, at least for low molecular weight CH_3-capped PEO, ether oxygen atoms near chain ends are not as effective for salt complexation as ether oxygen atoms near the center of the PEO chain. Therefore, we might expect that the salt solubility in CH_3-capped PEO will increase with increasing polymer molecular weight. This conclusion is in accord with the result of Raman spectroscopy studies by Torell[42] et al. of CH_3-capped PEO/$LiCF_3SO_3$ systems at EO/Li = 16:1 and $T > 270$ K, where a larger number of "free" ions was found for eight repeat unit PEO than for four (or less) repeat unit PEO.

Conclusions

In this paper, we have provided detailed information about the cation environment as well as changes in PEO chain conformations upon salt complexation in PEO/LiI system at 450 and 363 K. The results of our MD simulations agree well with the following experiments: (i) The local cation environment is in good agreement with NDIS experiments. (ii) The weak dependence of the local ion environment for salt concentrations less than EO/Li = 15:1 at 450 K is in accord with Raman spectroscopy studies on similar systems. (iii) The increase in the population of free ions with decreasing temperature observed in our simulations is in accord with a large number of Raman spectroscopy studies of polymer electrolytes. (iv) An increase in the populations of *tgt* and *tgg* conformations and a decrease in the populations of the *ttt* and *tgg′* conformations upon complexation are in good agreement with Raman and infrared studies.

The agreement between our MD simulations and experiments demonstrates the ability of our quantum-chemistry-based force field to reproduce many important features of polymer electrolyte systems. Accurate simulations can provide additional insight into mechanisms not available from experimental studies. For the dilute composition region (salt content less than EO/Li = 15:1) at 450 K we have found not only that the ion environment is nearly independent of salt concentration but moreover that salt-rich domains of PEO/LiI at least 11 Å in radius are formed and that their stoichiometry is also only slightly concentration dependent. Domains of PEO sequences, which consist of EO not having Li^+ in their first coordination shell (within 4.0 Å), behave structurally and conformationally like the pure PEO melt, having the same populations of conformational triads and the same spatial correlations as the pure PEO melt. This allows us to picture the PEO/LiI system as a mixture of PEO/LiI domains and PEO-like domains. However, at high salt composition (EO/Li = 5:1) the system at 450 K predominantly consists of PEO/LiI domains and essentially no identifiable PEO-like domains. In other words at EO/Li = 5:1 local heterogeneities disappear and the system becomes more homogeneous. With a temperature decrease from 450 to 363 K the size of the PEO/LiI domains in the EO/Li = 15:1 system decreases from 11 Å in radius to about 6−8 Å in radius.

In the PEO/LiI system at 450 K Li^+ cations were found to be predominately complexed by only one PEO chain, having from three to six contiguous EO in their first coordination shells. Complexation by longer sequences was found to be more probable at 363 K, as was complexation by more than one PEO chain. These phenomena were found to be largely entropically driven. Because of the conformational entropic penalty for long EO sequences to participate in complexation at high temperatures, the PEO chains are forced to adopt conformations that have less favorable PEO/Li^+ binding energy. This in turn allows I^- anions to more easily complex with Li^+ cations, resulting in a dramatic decrease in the probability of free ions from about 19% at 363 K to below 1% at 450 K for the EO/Li = 15:1 system. Note that the same phenomenon is also responsible for the decrease in the radius of gyration observed with decreasing temperature.

Acknowledgment. The authors are indebted to the National Science Foundation—Division of Materials Research for support provided through NSF CAREER award DMR 96-24475. We also would like to thank R. L. Jaffe and R. Boyd for helpful discussions and M. Woodson for help with system administration of our DEC Alphastations. An allocation of computer time from the Center for High Performance Computing at the University of Utah is gratefully acknowledged. CHPC's IBM SP system is funded in part by NSF Grant #CDA9601580 and IBM's SUR grant to the University of Utah.

References and Notes

(1) Ratner, M. A.; Shriver, D. F. *Chem. Rev.* **1988**, *88*, 109.
(2) Gray, F. M. *Solid Polymer Electrolytes. Fundamentals and Technological Applications*; VCH Publishers: New York, 1991.
(3) Gray, F. M. *Polymer Electrolytes*; The Royal Society of Chemistry: Cambridge, U.K., 1997.
(4) *Polymer Electrolyte Reviews*; MacCallum, J. R., Vincent, C. A., Eds.; Elsevier: New York, 1987; Vol. 1.
(5) *Polymer Electrolyte Reviews*; MacCallum, J. R., Vincent, C. A., Eds.; Elsevier: New York, 1989; Vol. 2.
(6) Lightfoot, P.; Mahta, M. A.; Bruce, P. G. *Science* **1993**, *262*, 883.
(7) Chatani, Y.; Fujii, Y.; Takayanagi, T.; Honma, A. *Polymer* **1990**, *31*, 2238.
(8) Chatani, Y.; Okamura, S. *Polymer* **1987**, *28*, 1815.
(9) Lightfoot, P.; Mehta, M. A.; Bruce, P. G. *J. Mater. Chem.* **1992**, *2*, 379.
(10) Robitaille, C. D.; Fauteux, D. *J. Electrochem. Soc.* **1986**, *133*, 315.
(11) Fauteux, D. In *Polymer Electrolyte Reviews*; MacCallum, J. R., Vincent, C. A., Eds.; Elsevier: New York, 1989; Vol. 2.
(12) Berthier, C.; Gorecki, W.; Minier, M.; Armand, M. B.; Chabagno, J. M.; Gigaus, P. *Solid State Ionics* **1983**, *9−10*, 1101.
(13) Frech, R.; Huang, W. *Macromolecules* **1995**, *28*, 1246.
(14) Frech, R.; Huang, W. *Solid State Ionics* **1994**, *72*, 103.
(15) Huang, W.; Frech, R.; Johansson, P.; Lindgren, J. *Electrochim. Acta* **1995**, *40*, 2147.
(16) Papke, B. L.; Ratner, M. A.; Shiver, D. F. *J. Phys. Chem. Solids* **1981**, *42*, 493.
(17) Muhuri, P. K.; Das, B.; Hazra D. K. *J. Phys. Chem. B.* **1997**, *101*, 3329.
(18) Schantz, S. *J. Chem. Phys.* **1994**, *94*, 6296.
(19) Schantz, S.; Sandahl, J.; Borjesson, L.; Torell, L. M.; Stevens, J. R. *Solid State Ionics* **1988**, *28*, 1047.
(20) Kakihana, M.; Schantz, S.; Torell, L. M. *J. Chem. Phys.* **1990**, *92*, 6271.
(21) Fretch, R.; Manning, J. P. *Electrochim. Acta* **1992**, *37*, 1499.
(22) Yoon, S.; Ichikawa, K.; MacKnight, J. W.; Hsu, S. L. *Macromolecules* **1995**, *28*, 4278.
(23) Berson, A.; Lindgren, J. *Solid State Ionics* **1993**, *60*, 37.
(24) Ferry, A. *J. Phys. Chem. B* **1997**, *101*, 150.
(25) Brodin, A.; Mattson, B.; Nilsson, K.; Torell, L. M.; Hamara, J. *Solid State Ionics* **1996**, *85*, 111.
(26) Reiche, A.; Tubke, J.; Siury, K.; Sandner, B.; Fleischer., G.; Wartewig, S.; Shashkov, S. *Solid State Ionics* **1996**, *85*, 121.
(27) Ferry, A.; Oradd, G.; Jacobsson, P. *Electrochim. Acta* **1998**, *43*, 1471.

(28) Carlsson, P.; Swenson, J.; McGreevy, R. L.; Gabrys, B.; Howelles, W. S.; Borjesson, L.; Torell, L. M. *Physica B* **1997**, *234−236*, 231.
(29) Londono, J. D.; Annis, B. K.; Habenschuss, A.; Borodin, O.; Smith, G. D.; Turner, J. Z.; Soper, A. K. *Macromolecules* **1997**, *30*, 7151.
(30) Vachon, C.; Vasco, M.; Perrier, M.; Prud'homme, J. *Macromolecules* **1993**, *26*, 4023.
(31) Vachon, C.; Labreche, C.; Vallee, A.; Besner, S.; Dumont, M.; Prud'homme, J. *Macromolecules* **1995**, *28*, 5585.
(32) Bergman, R.; Brodin, A.; Engberg, D.; Lu, Q.; Angell, A.; Torell, L. M. *Electrochim. Acta* **1995**, *40*, 2049.
(33) Bergman, R.; Borjesson, L.; Fytas, G.; Torell, L. M. *J. Non-Cryst. Solids*, **1994**, *172−174*, 830.
(34) Muller-Plather, F.; van Gunstreren, W. F. *J. Chem. Phys.* **1995**, *103*, 4745.
(35) Muller-Plather, F. *Acta Polym.* **1994**, *45*, 259.
(36) Neyertz, S.; Brown, D. *J. Chem. Phys.* **1996**, *104*, 3797.
(37) Boinske, P. T.; Curtiss, L.; Halley, J. W.; Lin, B.; Sutjianto, A. *J. Comput.-Aided Mater. Des.* **1996**, *3*, 385.
(38) Catlow, C. R. A.; Mills, G. E. *Electrochim. Acta* **1995**, *40*, 2057.
(39) Xie, L.; Farrington, G. C. *Solid State Ionics* **1992**, *53−56*, 1054.
(40) Neyerts, S.; Brown, D.; Thomas, J. O. *Electrochim. Acta* **1995**, *40*, 2063.
(41) Payne, V. A.; Xu, J. H.; Forsyth, M.; Ratner, M. A.; Shriver, D. F.; de Leeuw, S. W. *Electrochim. Acta* **1995**, *40*, 2087.
(42) Smith, G. D.; Yoon, D. Y.; Jaffe, R. L.; Colby, R. H.; Krishnamoorti, R.; Fetters, L. J. *Macromolecules* **1996**, *29*, 3462.
(43) Smith, G. D.; Borodin, O.; Pekny, M.; Annis, B.; Londono, D.; Jaffe, R. L. *Spectrochim. Acta A* **1997**, *53*, 1273.
(44) Jaffe, R. L.; Smith, G. D.; Yoon, D. Y. *J. Phys. Chem.* **1993**, *97*, 12745.
(45) Smith, G. D.; Jaffe, R. L.; Yoon, D. Y. *J. Phys. Chem.* **1993**, *97*, 12752.
(46) Smith, G. D.; Jaffe. R. L.; Partridge, H. *J. Phys. Chem. A* **1997**, *101*, 1705.
(47) Nose, S. *J. Chem. Phys.* **1984**, *81*, 512.
(48) Ryckaert, J. P.; Ciccotti, G.; Berendsen, H. J. C. *J. Comput. Phys.* **1977**, *23*, 327.
(49) Smith, G. D.; Yoon, D. Y.; Wade, C. G.; O'Leary, D.; Chen, A.; Jaffe, R. L. *J. Chem. Phys.* **1997**, *106*, 3798.
(50) Torell, L. M.; Schantz, S. in *Polymer Electrolyte Reviews*; MacCallum, J. R., Vincent, C. A., Eds.; Elsevier: New York, 1989; Vol. 2.
(51) Neyertz, S.; Brown, D. *Electrochim. Acta* **1998**, *43*, 1343.
(52) Salomon, M.; Xu, M.; Eyring, E. M.; Petrucci, S. *J. Chem. Phys.* **1994**, *98*, 8234.
(53) Torell, L. M.; Jacobsson, P.; Sidebottom, D.; Petersen, G. *Solid State Ionics* **1992**, *53−56*, 1037.

MA980838V